Electron ring accelerator with pulsed compression into a static field

W. Herrmann

IPP 0/15 June 1973

MAX-PLANCK-INSTITUT FÜR PLASMAPHYSIK

GARCHING BEI MÜNCHEN

MAX-PLANCK-INSTITUT FÜR PLASMAPHYSIK

GARCHING BEI MÜNCHEN

Electron ring accelerator with pulsed compression into a static field

W. Herrmann

IPP 0/15 June 1973

Die nachstehende Arbeit wurde im Rahmen des Vertrages zwischen dem Max-Planck-Institut für Plasmaphysik und der Europäischen Atomgemeinschaft über die Zusammenarbeit auf dem Gebiete der Plasmaphysik durchgeführt.

IPP 0/15 W. Herrmann

Electron ring accelerator with pulsed compression into a static field

Abstract

An electron ring accelerator is described that combines pulsed compression and static magnetic field acceleration. The model is calculated in detail, and an arrangement of coils is found that actually compresses rings into the static field system. Care has been taken to cross the coupling resonances at n = 0.2 and n = 0.1 with small growth rates. In addition, Landau damping coefficients for resistive-wall instabilities are calculated. The model uses 7 pulsed coils for compression and ring transport into the so-called "Wartesaal", a magnetic mirror, where the ring is kept to allow multiple ionization. One additional coil is needed for roll-out. The large number of coils does not pose a serious problem; the timing of the coils has only to be within a tolerance of ±100 ns.

A. Introduction

The first compressed rings with reasonable quality in the ERA-group Garching have been obtained with Kompressor I.[1] This was a fast compression scheme with three nested coil pairs. Rings could be compressed and loaded with ions, but there was no possibility to extract and accelerate them. This task was supposed to be done in Kompressor II, which in its design was an improved version of Kompressor I with addition of a single-turn coil expansion cylinder [2,3]. It turned out to be rather difficult to choose the position of the coils and their timing such that the radial component of the field B_r and its gradients in the actual position of the ring were adequate to the holding power and size of the ring, so far obtained. Although for larger holding powers Kompressor II seems applicable, it was not considered to be the best machine for early attempts of extraction and acceleration. For this purpose U. Schumacher developed his idea of the single turn coil, a combined compressor and accelerator, so-called "Schuko" [4]. One of the most striking properties of this compressor is its simplicity as far as electrical circuits are concerned. Because of the nearly homogeneous field inside the coil the B_r-component of the field and its gradients are small and well adapted to the holding powers achievable at present.

One of the major disadvantages of this arrangement seems to be its waste of energy in the large diameter coil and, connected with this fact, its unduly high costs if larger structures or higher repetition rates would be required. The cheapest way to get high fields in long structures seems to be by stationary currents in normal or superconducting coils. The static fields have the additional advantage that the rings can be kept by them for long ionization times.

The simplest and most interesting combination of a pulsed compressor and a stationary accelerator is given by the "sustained field" method as proposed for this purpose by C. Andelfinger [5]. In an early attempt to verify this idea it was shown by the author that by a suitable choice of the stationary coils and the shape of one pulsed coil it would be possible to compress rings in a field with the right focusing properties. Tolerances in the coil currents were 10^{-4}. The biggest problem, which seemed to give unsolvable difficulties was the field disturbance by the snout.

A solution to the task to combine a pulsed compression with a static acceleration has been found in the method, which is described in this paper. The main advantages of this scheme may be described as follows:

1) The static accelerator can be extended into relatively long structures. The techniques involved are well known and the energy dissipated can be minimized by the use of superconducting coils.

2) The static accelerator provides an easy method for a "Wartesaal", where the rings stay until the ions are in the desired state of ionization. This "Wartesaal" is necessary in fast compression schemes for acceleration of heavy ions.

The importance of possible disadvantages such as penetration of the pulsed field into the stationary coil and complications due to the large number of pulsed coils is discussed at the end of this report and is found to be not severe.

B. Pulsed compression into stationary acceleration

Instead of working with symmetric arrangements in order to get $B_r = 0$ for the desired position of the ring, in the proposed scheme the radial components of the static field are counteracted by the radial components of the pulsed field so that the surface where $B_r = 0$ continually moves and changes shape during the compression cycle. With the static field given it might be possible in principle to solve the problem by the addition of just one pulsed coil. But with one coil it seems rather difficult to achieve the desired field and field index contours, and the pulsed fields required to move the ring into the stationary field get unpractically high. It is therefore proposed to use a set of coils, where different coils not only provide compression and axial motion but also solve other tasks. Also in this way the energy in the pulsed system can be minimized, and the field index during compression can be controlled.

1) Stationary coil

Starting point of the calculation was the construction of a stationary magnetic field coil. Because the main aim of the present calculation was to show that and how it is technically possible to compress the ring and transfer it to a "Wartesaal", not very much attention was given to the accelerator part of the coil. The coil was chosen to be 86 cm long only with the "Wartesaal" about 18 cm from the compressor end. With the help of additional low power coils inside the main coil (not incorporated into the calculation) it seems possible to adjust the radial field strength in the accelerator part (B_r) to the holding power achieved in the ring, without changing the magnetic field in the compressor region considerably.

Fig. 1 shows the stationary coil as it is used in these calculation together with the B_z component of the field at R = 2.7 cm. In Fig. 2 B_r is plotted against the axial position z. The coil actually consists of two parts, divided by a slit, which provides the minimum in B_z for the "Wartesaal". In the calculations a current of 8 KA flows through the centers of crossectional elements of 2 x 2 cm^2 up to z = 80 cm. For larger z-positions a current of 16 KA flows through the center of elements 2 x 4 cm^2. For the determination of the fields this gave adequate accuracy. The ring will be kept at z = 58.4 cm (18.4 cm from the left end of the coil), almost independent on its radius. The field index at this position is rather small (n = 0.006 at R = 2.7 cm). If no other measures are taken, the ring spreads axially because of its selffield. A large axial spread however is undesirable for many respects. The time for example to ionize into higher states depends on the elctron flux density. The use of an additional focusing (e.g. squirrel cage) therefore seems to be necessary.

The first part of the stationary coil has an inner diameter of 20 cm. This appears to be rather large as far as energy consumption is concerned. But with a ring radius of 3 cm, squirrel cage, vacuum wall and spill-out coils it is not possible to reduce the diameter considerably. Going from 20 cm Ø to 16 cm Ø reduces the ohmic losses by about 20%, but increases heavily the difficulties to transfer the ring into the "Wartesaal". The second, much longer part of the coil has a smaller diameter of 16 cm, which eventually can be further reduced to about 12 cm.

2) Pulsed coils

After the decision has been made to operate with a set of pulsed coils instead of one coil, one can design the first coil with the main purpose of fulfilling the injection conditions. These were assumed to be the following:

Closed-orbit radius:	18 cm
Beam energy:	2 MeV
Field index n:	0.45

For radial inflection the field index should be closer to n = 0.55, but for axial inflection, which might be more practical in this case, n = 0.45 is more suitable for 3-turn inflection. In order to have some flexibility in the choice of the injection parameters without changing the position of the injection snout, the injection field should to a great part be determined by the first pulsed coil.

With the stationary coil positioned as shown in Fig. 3, proper injection conditions have been found at R = 18 cm, z = -14 cm for a position of coil 1 as indicated (R = 28 cm, $-32.5 \leq z \leq -28.5$ cm). The field index in this case is n = 0.453, and the energy of the electrons E = 2.229 MeV. The injection conditions can be changed by varying the radius or z-position of coil 1. Experimentally it is not easy to change the radius of a coil, but it is simple to move the coil axially. For a motion of the coil of 1 cm towards the stationary field the field index decreases by 3%, the injection energy increases by 0.7%. If the radius of the coil is increased by 1 cm, n gets lower by 7.7% and E increases by 3.2%.

At the injection closed orbit the radial components of the pulsed and stationary fields cancel each other. The total B_z-field is 499 Gauss, of which 301 Gauss is from the stationary field and 198 Gauss from the pulsed field. The compensation of the snout has to take both the static and the pulsed components into consideration.

Fig. 4 shows the lines of B_r = 10; 0; -10 Gauss around the injection closed orbit at injection time. The surface for B_r = 0 is not a plane as was expected; for the construction of an inflector this has to be taken into account. If the current in coil 1 is increased, the B_r = 0 line moves towards the stationary field.

The position of the 2nd coil can be chosen for the main purpose of crossing the Walkinshaw resonance (n = 0.2) with a negligible growth rate and of keeping the field index between 0.2 and 0.1 thereafter. The position of coil 2 and the other coils and of the screening elements can be seen in Fig. 3 and in Table I.

Table I

R_1	R_2	Z_1	Z_2	R	Z	N
Screening elements						
9.800	29.800	39.800	39.800	1.000	0.0	20
9.800	9.800	39.800	63.800	0.0	1.000	24
7.800	7.800	63.800	72.800	0.0	1.000	9
7.800	9.800	63.800	63.800	1.000	0.0	2
Compression coils						
28.000	28.000	-32.500	-28.500	0.0	1.000	4
19.500	21.500	- 6.500	- 3.500	0.500	0.750	4
16.000	18.000	13.500	16.500	0.500	0.750	4
13.000	13.000	24.000	27.000	0.0	0.750	4
8.000	10.000	31.000	35.000	0.500	1.000	4
6.500	6.500	39.500	41.900	0.0	0.400	6
6.000	6.000	56.500	62.500	0.0	0.857	7
6.000	6.000	54.000	54.800	0.0	0.400	2

Here (R_1, Z_1) and (R_2, Z_2) are the endpoints of the linear coil cross section. R and Z is the length of the subelements used in the program and N is the number of subelements for the coil in question. The dimension is cm.

Coil 3 has the same task for crossing n = 0.1 ($\nu_R - 3\nu_z = 0$) that coil 2 had with respect to n = 0.2. The 4th and 5th coils must keep the field index low and transport the ring into the stationary coil. These two coils could easily be combined to one coil, but energy considerations favored two separate coils. Coils 6 and 7 together accomplish the transport into the "Wartesaal".

While coil 7 compensates the "Wartesaal" temporarily, coil 6 presses the ring towards it and holds it there until the current in coil 7 is reduced to zero. The balance between coil 6 and coil 7 is rather delicate and is closely connected with the shape of the "Wartesaal".

Fig. 5 shows the radius R of the ring and its axial position z in cm, the field index n and the energy E in MeV as functions of time T in μs. Each coil serves to compress the ring in the radial direction and to move it axially at the same time. The axial motion at the beginning is about 1 mm for 3 turns, which is not nearly enough to clear the snout without a special system for inflection. The rate of radial compression is less than half the axial rate of motion.

In Fig. 6 the radius R and the field index n are plotted as functions of time for 3 different closed orbits at the time of injection: R = 19 cm, 18 cm, 17 cm. This spread in closed orbits corresponds to an energy spread of about $\pm$ 3%. The radial compression does not give any problems. The curves for the field index show that n = 0.2 and n = 0.1 are crossed rapidly for all energies. Growth rates for the Walkinsnaw resonance at n = 0.2 have been calculated by L.J. Laslett [6]. The same calculations for n = 0.1 have not been done because this resonance is expected to be harmless when the fields are symmetric with respect to the ring plane. Laslett finds for the n = 0.2 resonance that the total increase in axial amplitude (in decades) is:

$$G = 3.83 \cdot \frac{K^2 \cdot A_x^2}{|dn/d\tau|}$$

Here A_x is the ratio of the radial betatron amplitude to the major ring radius R, K is the coupling constant: $K = \frac{1}{2}\left[n^2 + n - R\frac{\partial n}{\partial R}\right]$ and $|dn/d\tau|$ is the rate of change of n per revolution. If we choose $A_x = 0.05$, we get the following G-values for the different starting radii:

R	17	18	19	cm
G	3×10^{-2}	2.44×10^{-2}	2.33×10^{-2}	decades

These growth rates are rather small. The increase in axial amplitude is 6%. Even with a twice as big a radial amplitude the increase in axial amplitude would be of the order of 25% only. For the n = 0.1 resonance, which is a higher order mode, the growth rates are hopefully not larger.

Although the resonances are crossed with small growth rates, n = 0.2 as well as n = 0.1 are approached closely more than once by the lower or higher energy electrons during compression. For example after firing coil 2 the field index approaches n = 0.1 and a few /us later n = 0.2. Depending on the magnitude of the selffields of the electron ring or the action of images, especially those in an axially focusing squirrel cage, one might like to change the field index trajectory so as to avoid resonances. The field index shortly after firing coil 2 can be increased by moving coil 2 in negative z-direction (closer to coil 1). On the other hand, if squirrel cage action dominates, a larger radius of coil 2 decreases the field index at the larger distances from the coil. The same is true for the other coils. Instead of moving the coil in negative z-direction and increasing the radius, the shape of the coil could be flared; that is, the radius of the coil could be increased with z. This would have both effects at the same time.

In the arrangement shown in Fig. 3 each of the coils 2, 3 and 5 is built with a flaring radius. This flaring is necessary in order to increase the radial component of the field close to each of these coils and to move the ring far enough in z-directions without unduly increasing the current in the preceding coil.

Coil 5 transports the ring into the stationary coil. Even before coil 6 takes over and carries the ring to the "Wartesaal", coil 7 is fired in order to fill up the field minimum. Coil 6 then moves the ring to the "Wartesaal" area, and the currents in coil 7 and all the other coils are reduced to zero. During the transport of the ring the field index n is kept positive,

although it sometimes assumes rather low values. By the use of more coils in the transport phase and a steeper mirror in the "Wartesaal" a larger field index could probably be obtained. But this would complicate roll-out and spill-out, and it therefore seemed to be the better way to rely on some kind of image forces (squirrel cage) for sufficient axial focusing.

In the "Wartesaal" the ring can be kept as long as necessary to get the desired degree of ionization. A coil 8 is already integrated into the system that could be used to initiate roll-out and to carry the ring beyond the middle of coil 7. If this coil were fired a second time, spill-out could be accomplished. Detailed calculations on this procedure have not yet been done, but major difficulties are not expected because of the availability of minor changes in the main field plus the possibility of help from an additional low field stationary coil.

In Fig. 7 the ring radius R and the field index n at the position of the ring are plotted as a function of z.

The change of the particle energy during compression can be found in Fig. 5. The total energy is roughly proportional to the square root of the axial field. Actually the ratio of the final energy to injection energy is 5.75, whereas the square root of the field ratio is 6.1 only. The difference is associated with the variation of the field index.

C. Miscellaneous

Single-particle resonances

Two of the more important single-particle coupling resonances (at n = 0.2 and n = 0.1) have been discussed earlier. There are quite a few other lower order resonances, which are crossed during compression. There are especially the three coupling resonances:

$$\nu_R - \nu_z \longrightarrow n = 0.5$$
$$3\nu_R - 4\nu_z \longrightarrow n = 0.36$$
$$\nu_R - 4\nu_z \longrightarrow n = 0.0588$$

Each of these modes can lead to growth without an external field perturbation. If the first mode at n = 0.5 gives trouble, it probably can be avoided - at least with axial inflection. Both of the other modes at n = 0.36 and n = 0.0588 involve higher orders and are hopefully not as destructive as the Walkinshaw-resonance.

Other resonances require external perturbations. Especially dangerous might be the resonances at n = 0.36, 0.25, and 0.11. The main disturbance in the field is probably due to the snout. The snout compensation therefore has to be rather good, and these resonances should be crossed far away from the snout. As it turns out n = 0.25 and n = 0.11 are crossed a few diameters of the snout away from it. The resonances $\nu_R + 2\nu_z = 2$ or $2\nu_R - \nu_z = 1$ at n = 0.36 could both be driven by snout perturbations and require for their nonappearance a good snout compensation.

Landau damping coefficients

Transverse resistive wall instabilities could be the origin of ring blow up inspite of a reasonable energy spread if the Landau damping coefficients are small. The calculation of the damping coefficients for the two first axial and radial transverse modes

has been included in the computation in the form given by L.J. Laslett [7]:

$$E\,\frac{\partial S_{R/z}}{\partial E} = \frac{1}{\beta^2}\left[\frac{R\cdot\frac{\partial n}{\partial R}}{2\nu_{R/z}^3\,[M-\nu_{R/z}]} - \left(\frac{1}{\nu_{R/z}^2} - \frac{1}{\beta^2}\right)\right]\cdot S_{R/z}$$

There $S_{R/z}$ is the frequency of the mode in question: $S_{R/z} = (M - \nu_{R/z})\cdot\omega_c$, with ω_c the gyrofrequency, $\nu_{R,z}$ the radial or axial tune, and E the particle energy.

As can be seen from a paper by G.R. Lambertson and L.J.Laslett [8] the growth rate ω_i is nearly proportional to the frequency $S_{R,z}$, if geometry, particle number and energy are constant. We therefore take the factor in brackets as a figure of merit. If its absolute value is much smaller than 1, then Landau damping might be undesirably small, even with relatively large energy spreads. Fig. 8 gives this factor for the different modes as a function of time during compression. On Fig. 9 the corresponding frequencies are plotted. The axial modes always have a figure of merit greater than 1. The situation is different for the radial modes. At the first sight it seems to be worst for the first radial mode. Here the damping factor gets below 1 a few times and even crosses zero during the transport phase. The first two minima below 1 occur shortly after firing coils 3 and 4. If experimentally an instability is found during these times, the damping factor could be increased by moving the coils to smaller z-positions, or by firing the coils only after the ring passed them by a greater distance than in the calculated example. This could be achieved by increasing the capacity in the circuits of coils 2 and 3. The next very steep minimum is found after firing coil 6. Here the same remedy might be applied. On the other hand the damping factor is really low only for about 70 ns. And as can be seen from Fig. 9, the corresponding frequency fR1 is only about 12 MHz, that is its period is comparable with the time that the damping is low, so that only for very large growth rates an appreciable growth should be expected. The same is true both at the next minimum (at 31 µs) and at the zero crossings

(near 35 μs), where the frequencies are 3 MHz and 1 MHz respectively. There is another reason why no great care has been taken to avoid these low values. Because of the very small field indices in the transport region some kind of additional external focusing has to be applied, which surely alters the Landau damping in this area. Thus in spite of the fact that the damping of the first radial mode looks bad, the more dangerous mode might be the second radial mode during the first few μs after injection. In this case if the radius of injection is reduced - as has been done in these calculations - the damping factor for the second radial mode increases remarkably. Conversely, for larger injection closed orbits the curve even crosses the zero line. The frequency fR2 in this case is high. The growth rates are not known. If an instability is found in the experiment, it might be necessary to change the geometry in order to reduce the growth rate. Altogether the situation did not seem to be dangerous enough to warrant the pursuit of a new series of runs with different coil settings.

Negative-mass instability

As is well known [9], the negative-mass instability imposes a serious limitation on the optimum qualities of the electron rings. The more favorable mechanism for suppressing negative-mass instabilities besides Landau damping is the use of conducting walls close to the ring [10]. In the case described here an inner conical cylinder could be brought close to the ring. As a necessary condition its conductivity would have to be adjusted so that the fields of the pulsed coils could penetrate, while simultaneously the high frequency fields of the instability still see a good enough conductor. In addition to the suppression of negative-mass instability, this cylinder could provide some axial focusing for one of the following reasons: If the ring moves faster than the image currents decay, then at least the toroidal effect is reduced. Or on the other hand, if the image currents decay faster, then the cylinder acts like a squirrel cage.

This type of inner cylinder could be used only as long as the self-field energy of the ring is not a great fraction of its kinetic energy, because if it were, then the energy losses during the penetration of the rings magnetic field into the cylinder would be too large.

(Although prevention of the negative-mass instability might be possible by means of neighbouring conducting walls, the necessary condition of lossy walls in all fast compression schemes (for penetration of the main field) imposes a severe limitation because of the enhancement of transverse resistive-wall instabilities. A somewhat slower compression might be the only way out of this difficulty, if the growth of single-particle resonances can be kept small.)

Use of squirrel cages

During the compression of the ring into the stationary coil the external focusing is always sufficient. But during the transport of the ring inside the coil to the "Wartesaal" the field index gets rather low and because of the linear or toroidal effects of the self-field the ring might loose its axial integrity. In the form given by L.J. Laslett [11] we find for the linear and toroidal effect with no ions present and a = b = 0.1 cm, R = 3 cm, γ = 30 and $N_e = 10^{13}$:

$$|\Delta n_{linear}| = + 0.01$$
$$|\Delta n_{toroidal}| = + 0.027$$

The linear term acts defocusing in either direction, the toroidal effect is defocusing in axial and focusing in radial direction. Image charges on cylinders outside or inside the ring however are focusing in axial and defocusing in radial direction. This term is given by:

$$|\Delta n_{squirrel\ cage}| = \pm 4 \frac{\varepsilon_{1E}}{(\varepsilon_E - 1)^2}$$

Here S_E is the ratio of squirrel-cage radius to ring radius, and $\varepsilon_{1E} = 0.125$ [12]. If the squirrel-cage is only 4 mean minor radii away from the ring as assumed in [10] for suppression of negative-mass instability, then we get with the above mentioned data:

$$|\Delta \nu_{\text{squirrel cage}}| = 0.138$$

This value is by far sufficient to cancel the effect of the ring self-field. Its distance from the ring can be enlarged, if its structure is different from the negative-mass cylinder.

If the squirrel cage focusing could be used in the accelerator part also, the number of ions in the ring would no longer be determined by the necessary focusing, but could be made deliberately small. This way the threshold in the maximum holding power for ion-electron instabilities as calculated by [13,9] can be increased at least until the limitation set by negative-mass is reached. For some experiments a smaller number of ions per pulse might be tolerable if at the same time the energy gain per meter is increased.

Technical aspects

Each pulsed coil was assumed in the calculation to be connected to a circuit whose schematic diagram was as follows:

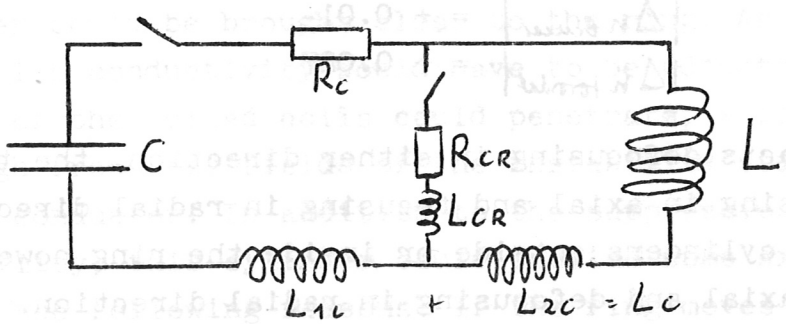

A condenser is discharged through the coil inductance L via a resistance R_c and a circuit inductance L_c. At current maximum the crowbar switch is closed in the crowbar circuit with L_{cR} and R_{cR}. The capacities are assumed to be multiples of the standard

size of 8.4 µF. The condensers for coils 1 to 6 are charged to U = 30 KV. Table II in Fig. 10 presents the values for the circuit elements together with their firing times T_1 and crowbar times T_2.

The total energy stored in the condensers for the first 6 coils is 49.2 kJ. The crowbar resistances are relatively large in order to reduce the currents through the coils as fast as possible. This is necessary in order to avoid penetration of the pulsed fields into the stationary coil.

In table III in Fig. 10 the self and mutual inductances L_{MN} of the coils are listed that are obtained in the presence of the shielding "Dosen". (These shielding elements shall prevent penetration of the pulsed fields into the stationary coil, as is discussed later.) The negative values of a few mutual inductances for far away elements indicate the accuracy of the program. The real values of these mutual inductances are about 5 orders of magnitude smaller than the smallest self inductance and are therefore unimportant for the determination of the currents in the coils. The general accuracy is of the order 10^{-4}.

The current through the coils as a function of time is shown in Fig. 11. The highest currents of about 200,000 A are obtained in coil 5. At the edges of the coil the surface current density reaches values of about 100 KA/cm. About the same value is reached at the edges of coil 6.

One major problem connected with a multicoil arrangement could arise from small tolerances in firing- and crowbar-times of the different coils. From different program runs however it turned out that it was sufficient when the time jitter was within $\pm$100 ns.

Penetration of the pulsed field into the main coil

One of the most serious problems with the system of a pulsed compressor and a stationary accelerator is the penetration of the pulsed fields into the multiwinding stationary coil because of two reasons: 1. when the field penetrates the shielding, the field distribution deviates from the one calculated, and consequently ring transport might no longer be possible; 2. high voltages might be induced in the stationary coil that could lead to break-downs.

The stationary coil therefore has to be enclosed in a good conducting metal box and the crowbar circuits of the coils have to be damped. If we look at the currents of Fig. 11 we might choose 1 KHz as a lower limit for the frequencies involved. The equivalent thickness of the current layer in Cu then is: s = 0.2 cm. If we take the shielding sheaths used in the calculation (see table I and Fig. 3) as the medium plane of the copper sheath, then thicknesses up to 0.4 cm could be used, which would be in agreement with these calculations. Such sheaths would certainly exclude the pulsed fields from the stationary coil.

D. Summary

An electron ring compressor is proposed and in some detail calculated that makes use of pulsed compression and static acceleration. It is shown that it is possible to compress rings into a "Wartesaal" of the static coil. The advantages of the system are a relatively fast compression with rapid crossing of dangerous resonances combined with the possibility to keep the ring in the compressed state before roll-out as long as it is necessary for multiple ionization. Static fields for acceleration have the advantage of lower costs, especially if high repetition rates are required. Possible disadvantages are not considered to be serious. Problems connected with collective instabilities are not different in this geometry from those in existing fast compression schemes.

Acknowledgement

Part of this work was done during the author's visit in the ERA-group of the Lawrence Berkeley Laboratory, whose hospitality is gratefully acknowledged. Many discussions with my colleagues, especially M. Ulrich, helped to clarify the technical aspects. My thanks go to Dr. C. Andelfinger and J. Peterson for critically reading the manuscript.

References

1 See for example: C. Andelfinger et al., Status report on electron ring experiment in Garching. Proc. 4. Work Meeting on electron ring accelerators, 1971, IPP 0/3

2 W. Herrmann, unpublished (see Monatl.Mitteilungen 33, Mai/Juni 1970)

3 A.U. Luccio, Proc. 4. Work Meeting on electron ring accelerators, 1971, IPP 0/3, page 63, W. Dommaschk, unpublished

4 U. Schumacher, IPP 0/10, March 1972

5 C. Andelfinger, private communication

6 L.J. Laslett, ERAN 71, March 1970

7 L.J. Laslett, ERAN 126, February 1971

8 G.R. Lambertson, L.J. Laslett, ERAN 157, July 1971

9 D. Möhl, L.J. Laslett, A.M. Sessler, Proc. Symposium on collective methods of acceleration, Dubna, Sept. 1972

10 A. Faltens, L.J. Laslett, Proc. Symposium on collective methods of acceleration, Dubna, Sept. 1972

11 L.J. Laslett, ERAN 30, April 1969

12 A.U. Luccio, ERAN 35, June 1969

13 P.R. Zenkevich, D.G. Koshkarev, Particle accelerators 3, 1, (1972)

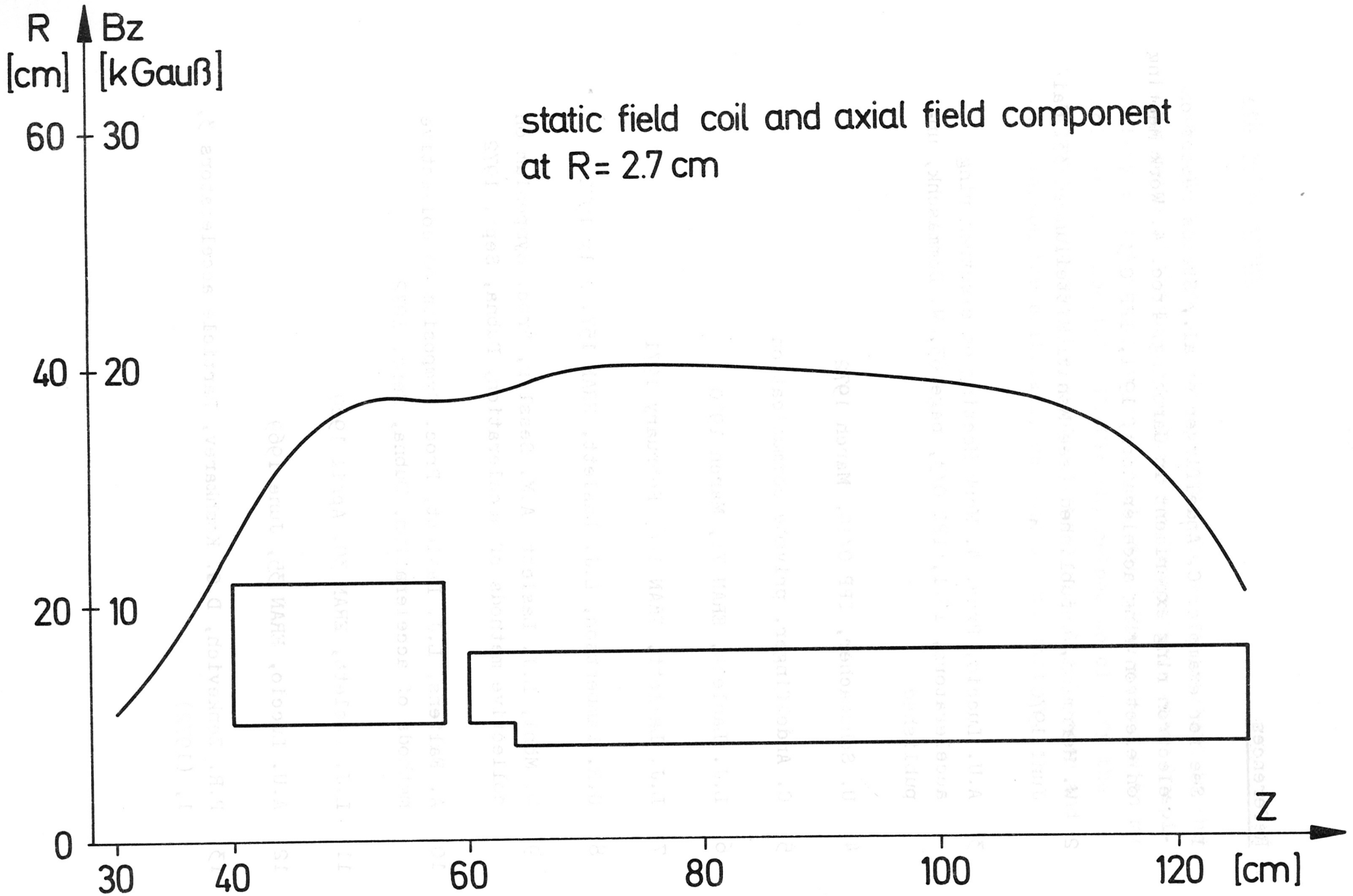
R [cm]
Bz [kGauß]
60
30
40
20
20
10
0
30
40
60
80
100
120 [cm]
Z
static field coil and axial field component
at R= 2.7 cm

Fig. 1

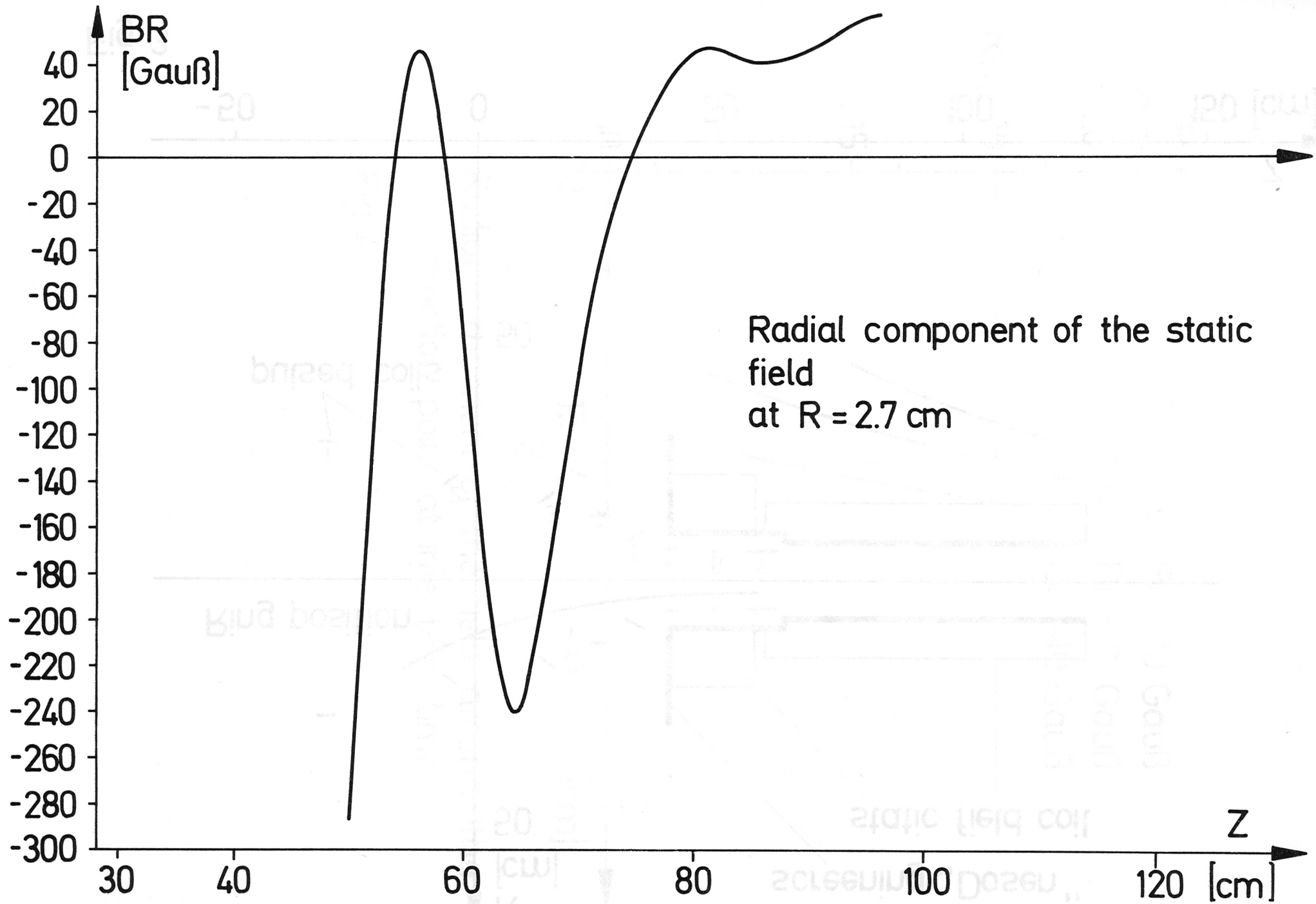
BR
[Gauß]
40
20
0
-20
-40
-60
-80
-100
-120
-140
-160
-180
-200
-220
-240
-260
-280
-300
30
40
60
80
100
120
[cm]
Z
Radial component of the static field
at R = 2.7 cm

Fig. 2

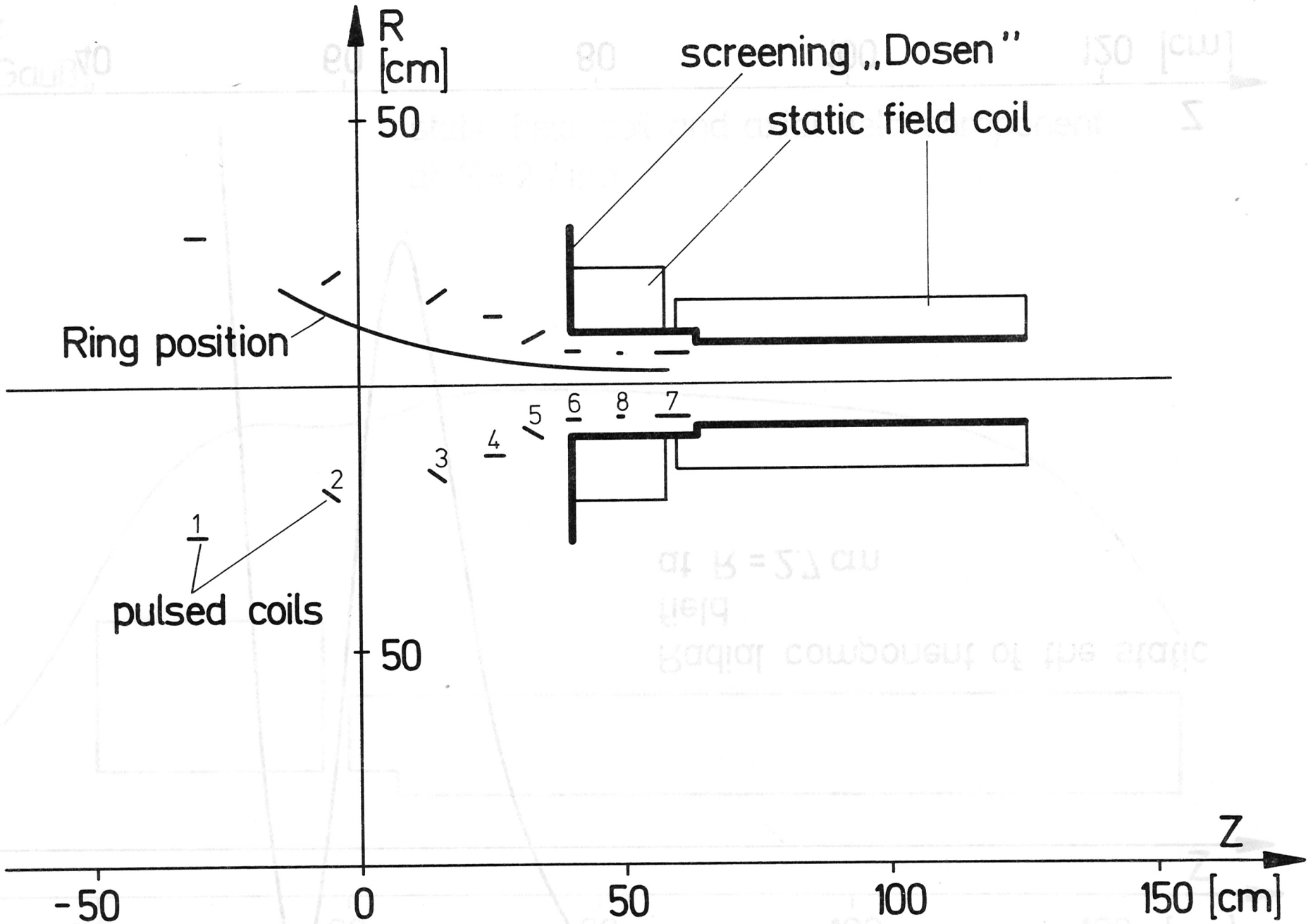
R
[cm]
50
screening „Dosen"
static field coil
Ring position
6
8
7
5
4
3
2
1
pulsed coils
50
Z
-50
0
50
100
150 [cm]

Fig. 3

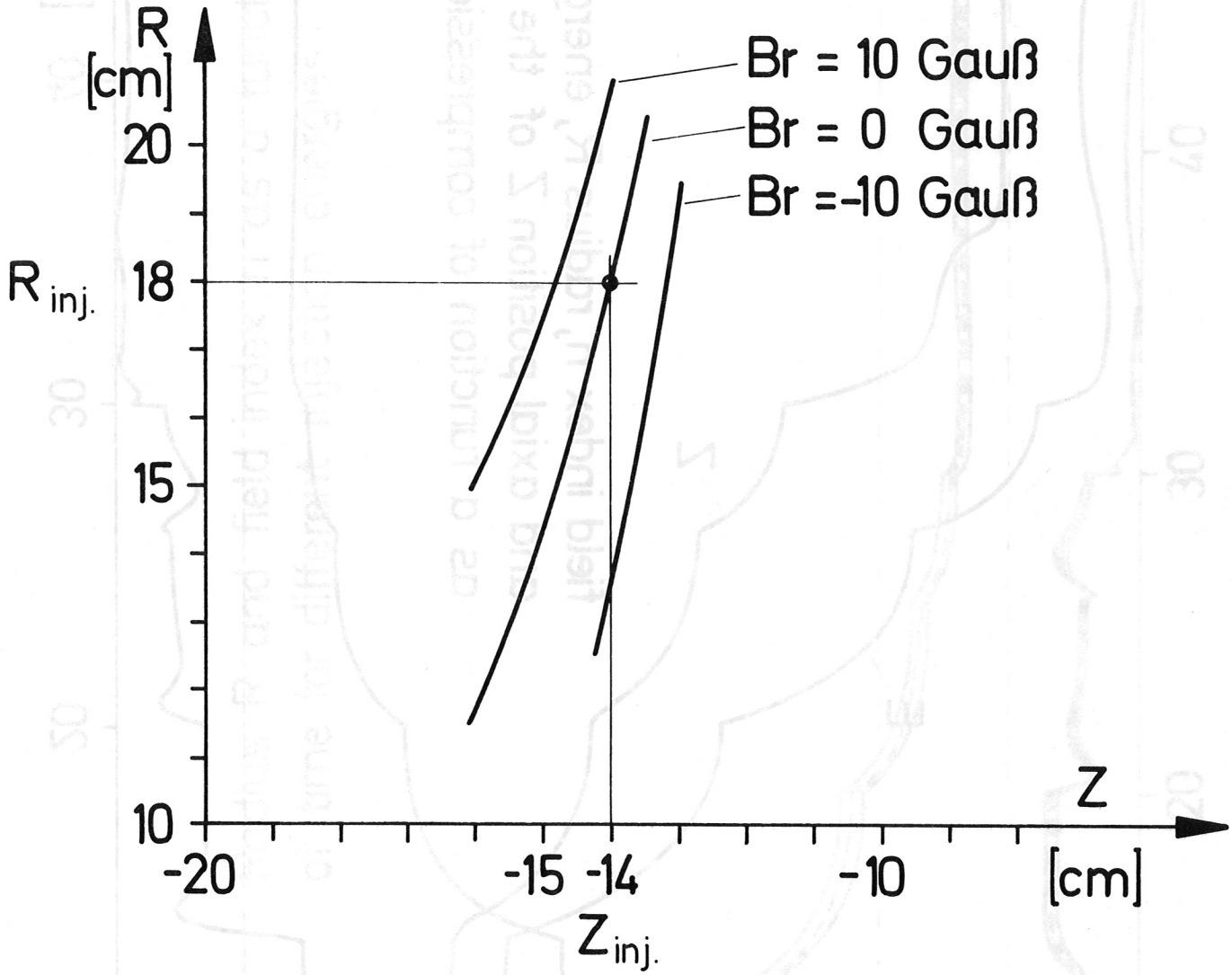

Radial component of the field around the injection point at injection time

Fig. 4

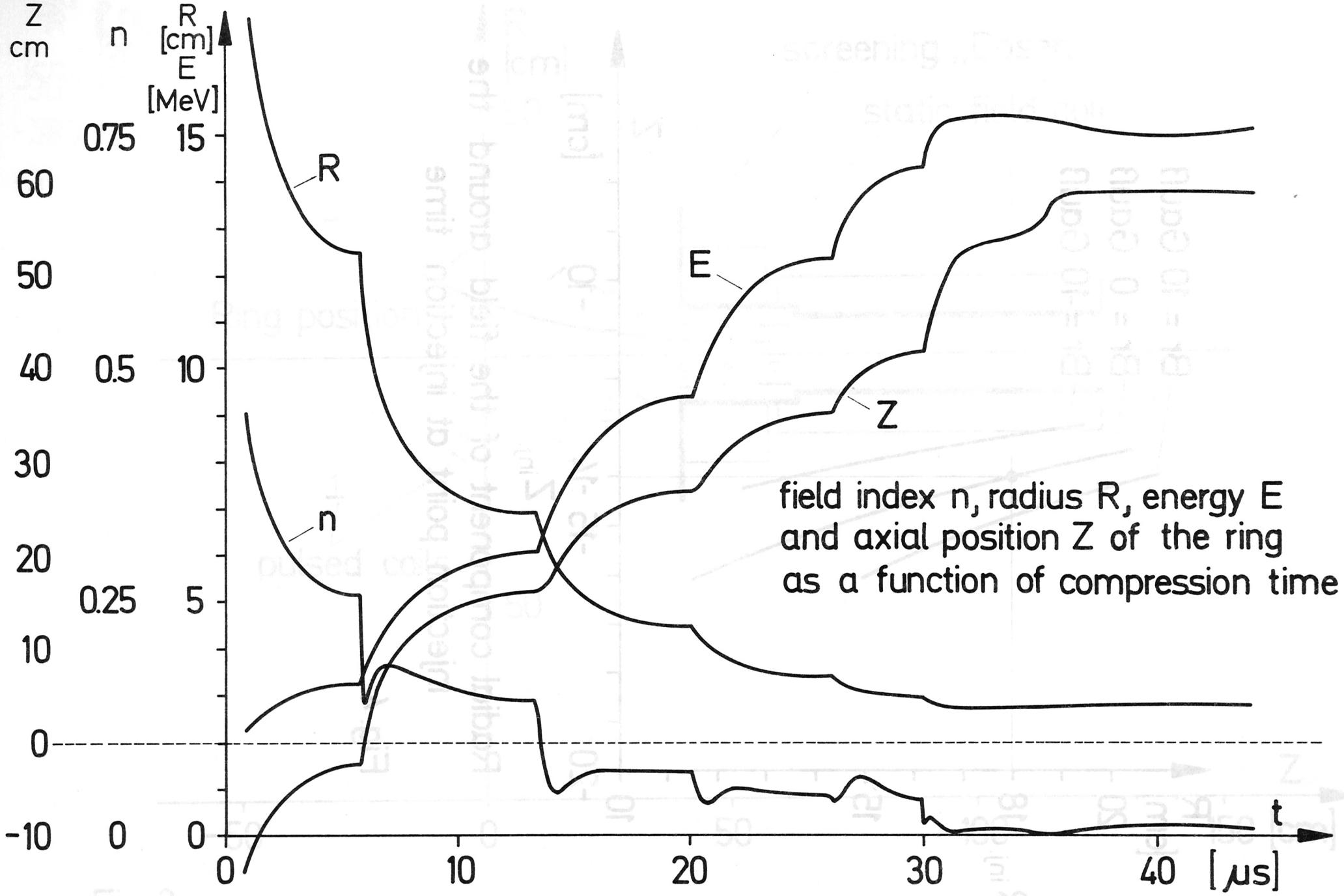

field index n, radius R, energy E and axial position Z of the ring as a function of compression time

Fig. 5

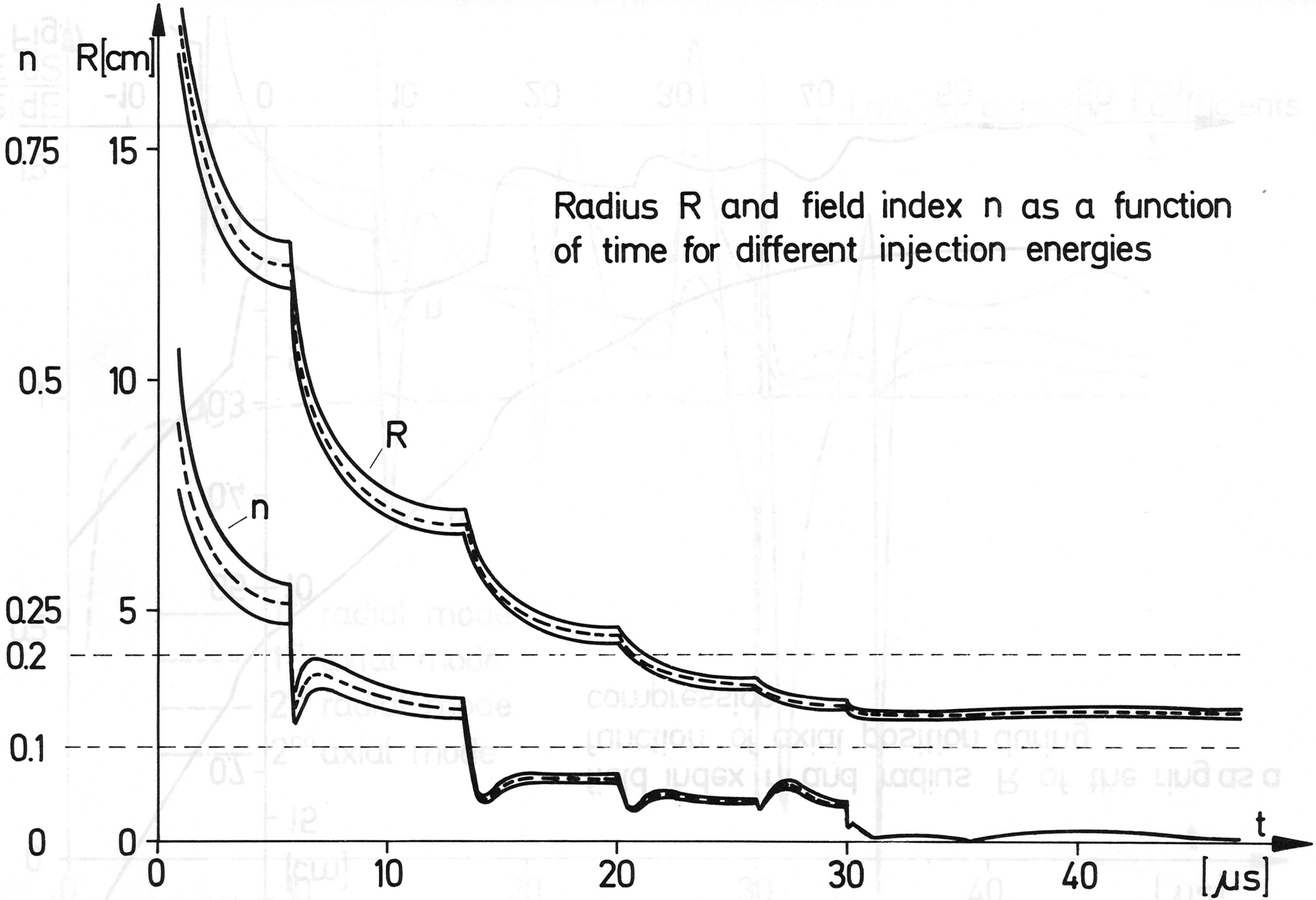

Radius R and field index n as a function of time for different injection energies

Fig. 6

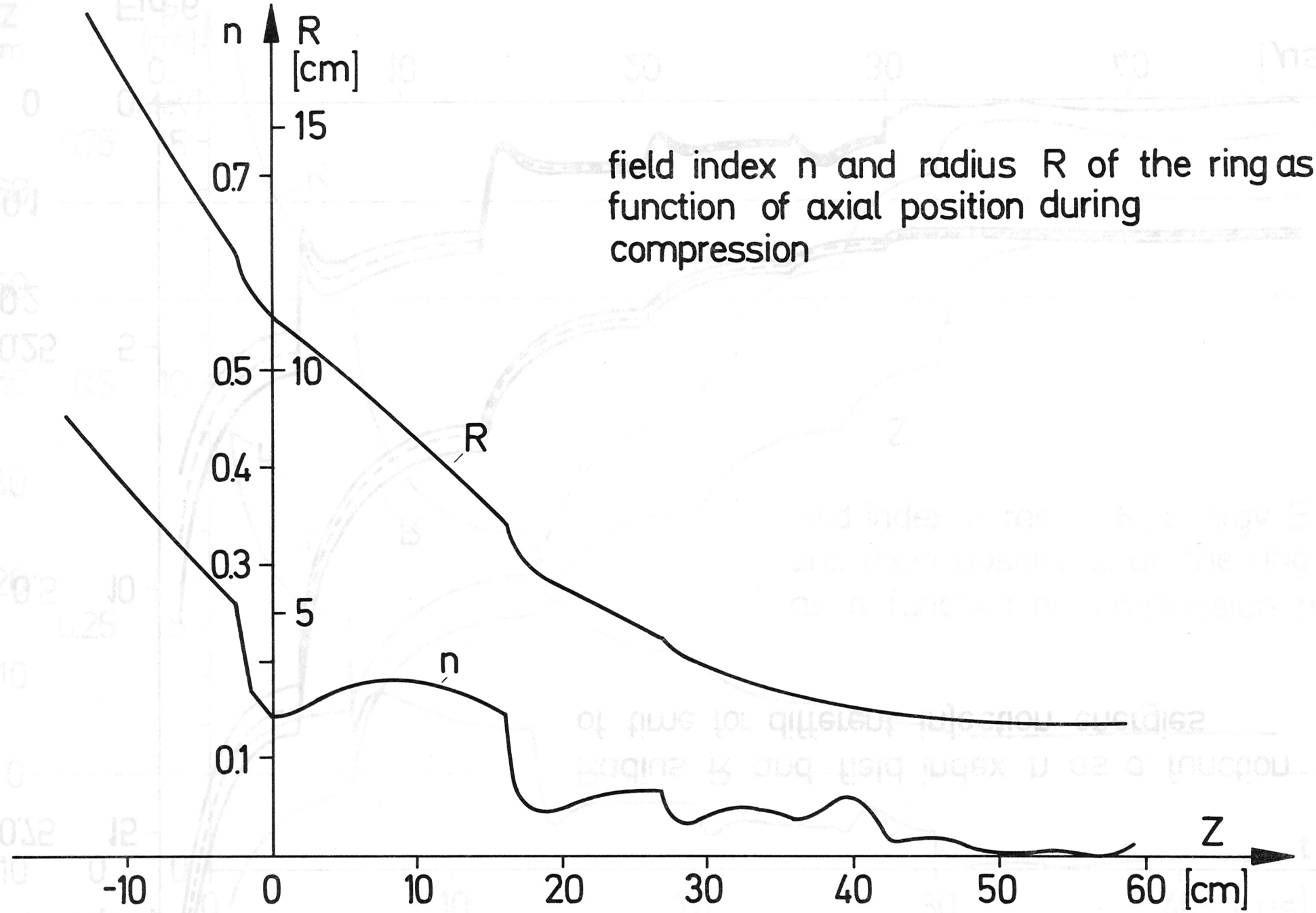

field index n and radius R of the ring as a function of axial position during compression

Fig. 7

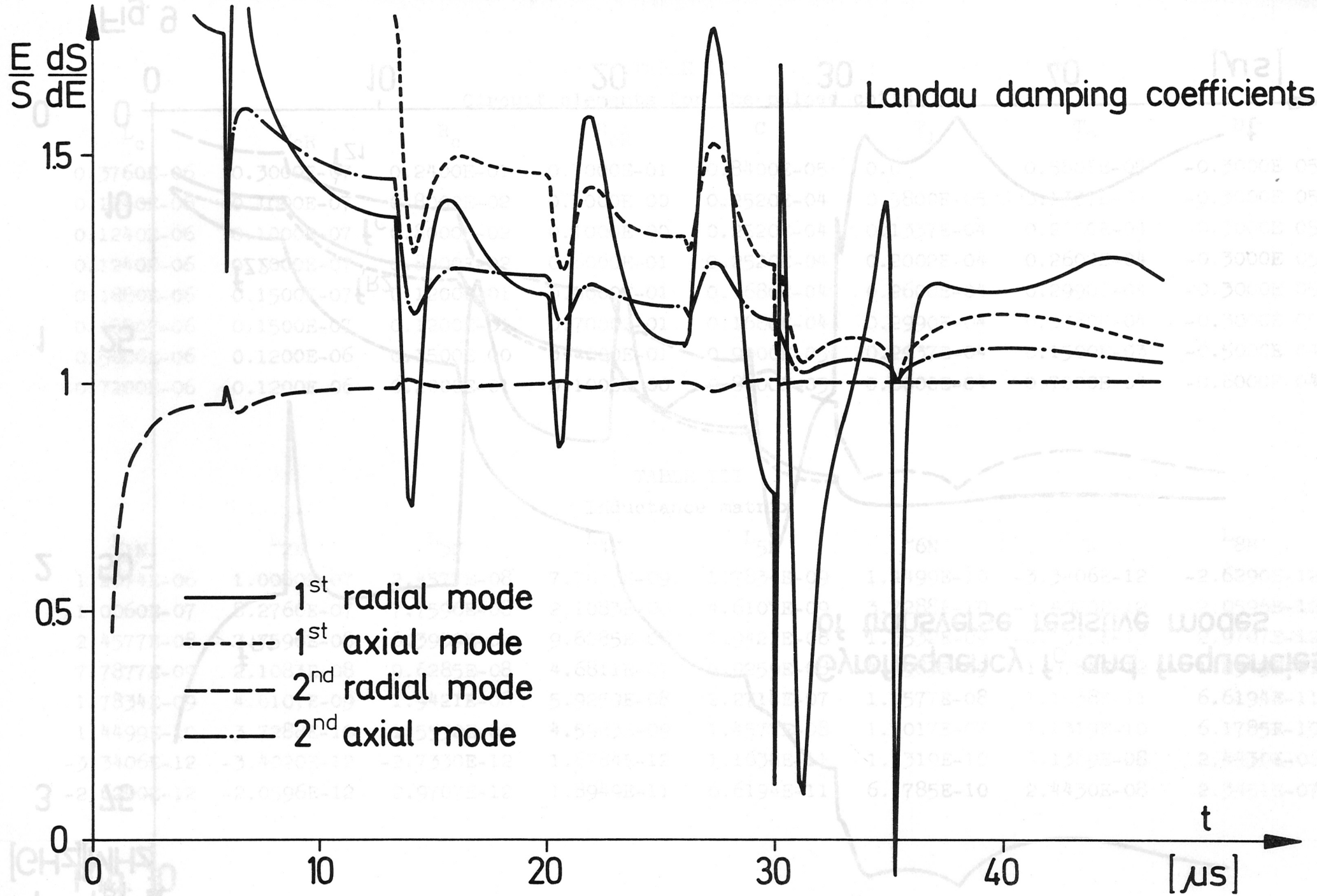
Landau damping coefficients
E dS / S dE
1.5
1
0.5
0
0
10
20
30
40
t
[μs]
1st radial mode
1st axial mode
2nd radial mode
2nd axial mode

Fig. 8

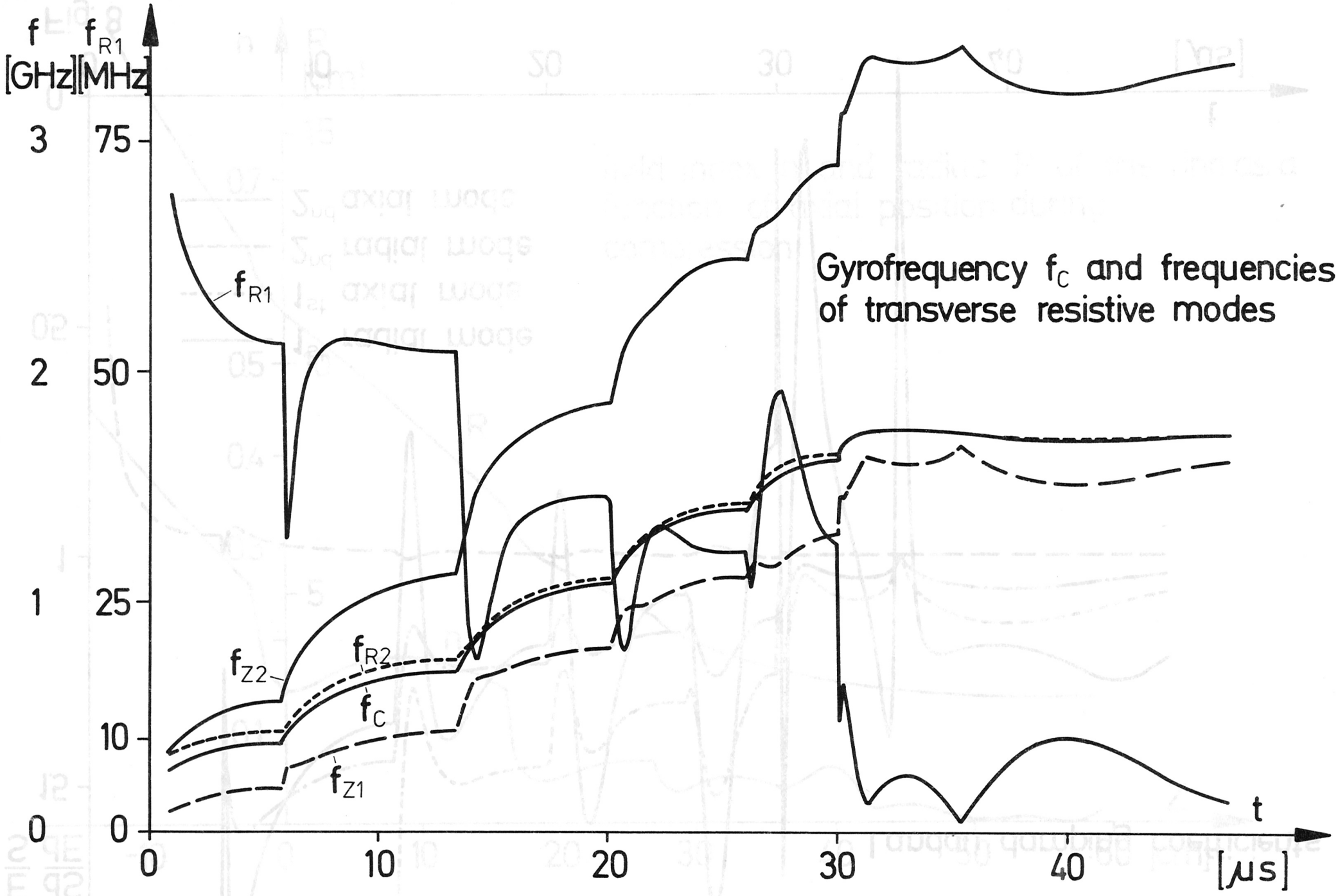
f [GHz]
f_R1 [MHz]
3
75
2
50
1
25
0
0
10
0
10
20
30
40
[μs]
t
f_R1
f_R2
f_Z2
f_C
f_Z1
Gyrofrequency f_C and frequencies
of transverse resistive modes

Fig. 9

TABLE II

Circuit elements for the pulsed coils

L_c	L_{cR}	R_c	R_{cR}	C	T_1	T_2	U
0.3760E-06	0.3000E-07	0.2400E-01	0.7000E-01	0.8400E-05	0.0	0.5801E-05	-0.3000E 05
0.1240E-06	0.1000E-07	0.8000E-02	0.1000E 00	0.2520E-04	0.5800E-05	0.1337E-04	-0.3000E 05
0.1240E-06	0.1000E-07	0.8000E-02	0.1000E 00	0.2520E-04	0.1337E-04	0.2000E-04	-0.3000E 05
0.1240E-06	0.1000E-07	0.8000E-02	0.6000E-01	0.2520E-04	0.2002E-04	0.2602E-04	-0.3000E 05
0.1880E-06	0.1500E-07	0.1200E-01	0.5000E-01	0.1680E-04	0.2600E-04	0.2990E-04	-0.3000E 05
0.1880E-06	0.1500E-07	0.1200E-01	0.7000E-01	0.1680E-04	0.2990E-04	0.3380E-04	-0.3000E 05
0.5000E-06	0.1200E-06	0.1500E 00	0.4000E-01	0.9000E-05	0.2937E-04	0.1500E-03	-0.5000E 04
0.7200E-06	0.1200E-06	0.2000E-01	0.1000E 00	0.8400E-05	0.6000E-04	0.7000E-04	-0.6000E 04

TABLE III

Inductance matrix

L_{1N}	L_{2N}	L_{3N}	L_{4N}	L_{5N}	L_{6N}	L_{7N}	L_{8N}
1.2074E-06	1.0060E-07	2.4577E-08	7.7877E-09	1.7834E-09	1.4499E-10	-3.3406E-12	-2.6290E-12
1.0060E-07	8.2766E-07	7.7596E-08	2.1083E-08	4.6107E-09	3.7288E-10	-3.4020E-12	-2.0596E-12
2.4577E-08	7.7596E-08	6.3939E-07	9.6285E-08	1.9421E-08	1.5532E-09	-2.7330E-12	2.9707E-12
7.7877E-09	2.1083E-08	9.6285E-08	4.6811E-07	5.9259E-08	4.5983E-09	1.6784E-12	1.8949E-11
1.7834E-09	4.6107E-09	1.9421E-08	5.9259E-08	2.2718E-07	1.4577E-08	1.1638E-11	6.6194E-11
1.4499E-10	3.7288E-10	1.5532E-09	4.5983E-09	1.4577E-08	1.7017E-07	1.1319E-10	6.1785E-10
-3.3406E-12	-3.4020E-12	-2.7330E-12	1.6784E-12	1.1638E-11	1.1319E-10	9.1389E-08	2.4430E-08
-2.6290E-12	-2.0596E-12	2.9707E-12	1.8949E-11	6.6194E-11	6.1785E-10	2.4430E-08	2.3451E-07

Fig. 10

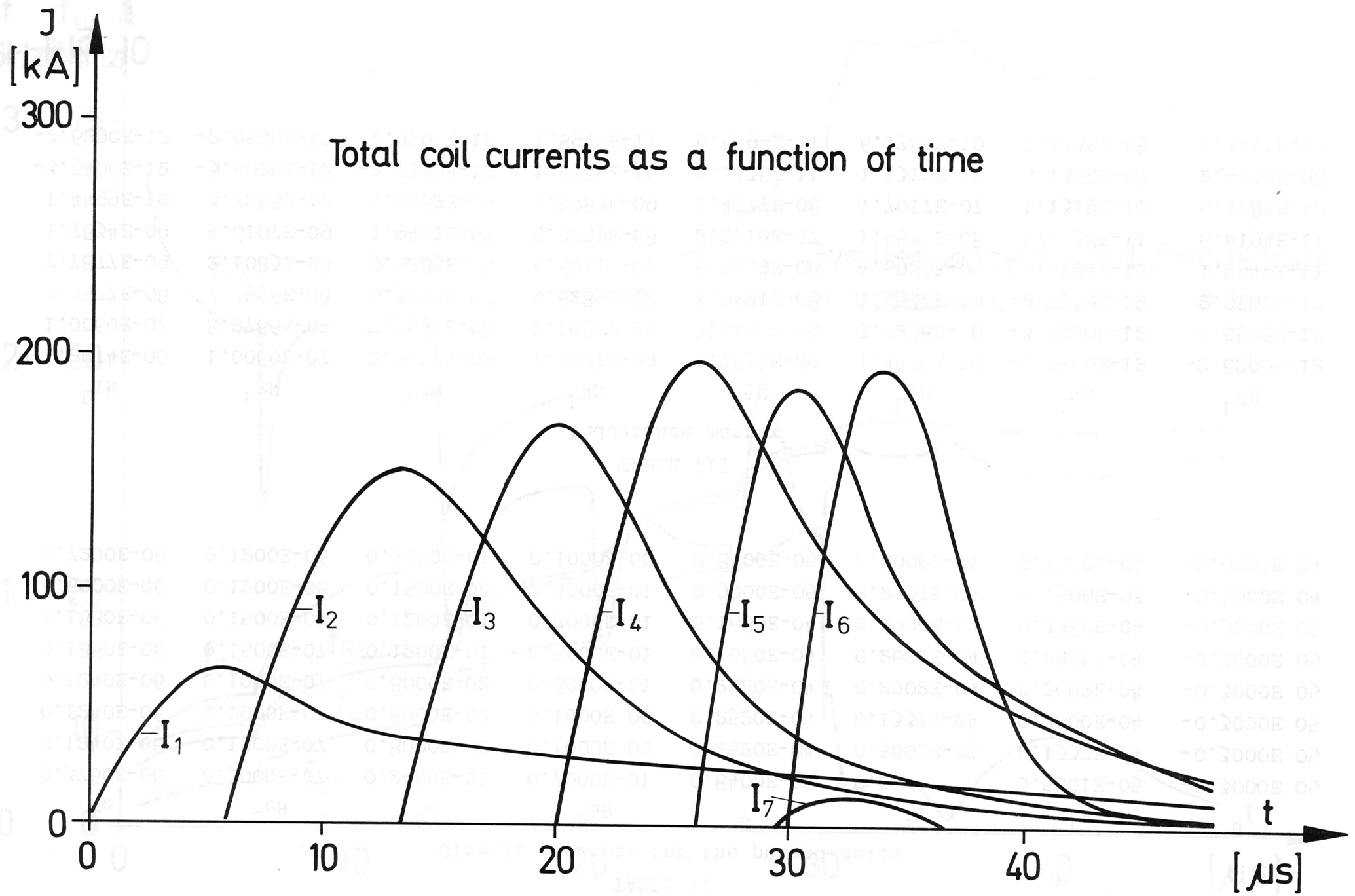
J
[kA]
300
200
100
0
Total coil currents as a function of time
I_1
I_2
I_3
I_4
I_5
I_6
I_7
t
0
10
20
30
40
[μs]

Fig. 11